MRS Advances © 2017 Materials Research Society
DOI: 10.1557/adv.2017.305

Lead-free $BaTiO_3$ Nanowire Arrays-based Piezoelectric Energy Harvester

Changyeon Baek,[1] Hyeonbin Park,[2] Jong Hyuk Yun[1], Do Kyung Kim[1] and Kwi-Il Park[2*]

[1]Department of Materials Science and Engineering, Korea Advanced Institute of Science and Technology (KAIST), 291 Daehak-ro, Yuseong-gu, Daejeon, 34141, Republic of Korea
[2]Department of Energy Engineering, Gyeongnam National University of Science and Technology (GNTECH), 33 Dongjin-ro, Jinju-si, Gyeongsangnam-do, 52725, Republic of Korea

ABSTRACT

Vertically aligned $BaTiO_3$ nanowire (NW) arrays on a Ti substrate were adopted for use in piezoelectric energy harvesting device that scavenges electricity from mechanical energy. $BaTiO_3$ NWs were simultaneously grown at the top and bottom surfaces of a Ti substrate by two-step hydrothermal process. To characterized the piezoelectric output performance of the individual NW, we transferred a $BaTiO_3$ single NW that was selected from well-aligned NW arrays onto a flexible substrate and measured the electric signals during the bending/unbending motions. For fabricating a piezoelectric energy harvester (PEH), both NW arrays were sandwiched between two transparent indium tin oxide (ITO)-coated polyethylene terephthalate (PET) plastic films and then packaged with polydimethylsiloxane (PDMS) elastomer. A lead-free $BaTiO_3$ NW array-based PEH produced an output voltage of about 90 V and a maximum current of 1.2 μA under periodically bending motions.

INTRODUCTION

Energy conversion technologies that harvest electric energy from sustainable energy resources (e.g., solar, thermal, wind, and mechanical energies) have attracted attention as alternatives to resolve the environmental problems and exhaustion of energy resources faced by our society [1-2]. Among these renewable energy resources, mechanical energy (such as vibration, bending, pressure, and stretching) sources, which are more accessible harvesting resources compared to other ambient energies, are being studied with great interest in attempts to achieve the energy harvesting without any limitation [3-4]. To convert the mechanical energy provided by nature, industry, and even humans into electric energy, many researchers have used piezoelectric materials, for example, wurtzite-structured ceramics (ZnO [5-8], ZnS [9], CdS [10], and GaN [11]) and perovskite-structured ceramics [$BaTiO_3$ [12], $PbZr_xTi_{1-x}O_3$ (PZT)[13], and $(1-x)Pb(Mg_{1/3}Nb_{2/3})O_3–xPbTiO_3$ (PMN–PT) [14]], and proposed piezoelectric energy harvesters (PEHs) that can generate output voltage and current signals during repeated mechanical deformation. Wang and co-workers characterized the individual piezoelectric outputs of a ZnO single NW [7] and demonstrated the aligned ZnO nanowire (NW) arrays-based flexible PEH technology in response to demand of the flexible, wearable, and permanent energy generation devices [8]. Although they provided the possibility that one-dimensional (1D) piezoelectric NWs can be used for realizing flexible PEHs, the output performance that they achieved is not satisfactory for operation of commercial electronics because of the lower piezoelectric properties of these materials compared to those of perovskite-structured ceramic materials.

In this study, we vertically grown the lead-free $BaTiO_3$ NW arrays on a thin Ti substrate by a simple low temperature hydrothermal reaction method and characterized the output performance generated from the $BaTiO_3$ NW-based high-output flexible PEH. In addition, we investigated the piezoelectric energy production ability of an individual $BaTiO_3$ single NW by transferring NWs selected from well-aligned NW arrays onto a flexible substrate and connecting both ends of a single NW to Au electrode pads to measure the electric signals. During periodic deformation by a bending machine, a $BaTiO_3$ single NW converted output voltage from 6 to 10 mV and current peaks from 1.0 to 2.3 nA. When a lead-free $BaTiO_3$ NW array-based PEH was stressed by human fingers, the output voltage and current values reached to 90 V and 1.2 μA, respectively.

EXPERIMENT

Synthesis of $BaTiO_3$ NW arrays on a Ti substrate

$BaTiO_3$ NW arrays on a Ti substrate were approached via a widely-used two-step hydrothermal reaction. The first step was to align sodium titanate NW arrays on a Ti substrate as intermediate structures. The Ti substrate (Sigma-Aldrich, 99.7 %, 127 μm thick) was oxidized at 600 °C for 6 hr and immersed in a Teflon-autoclave filled with 10 M NaOH solution. Next, the sealed reactor was maintained at a temperature of 200 °C in an oven for 16 hr. The resulting substrate obtained from the autoclave were washed with deionized water/alcohol four times and then dried at room temperature. For converting this structure into $BaTiO_3$ NW arrays via ion exchange reaction, the as-synthesized reactant was poured into a Teflon bottle with a barium source [0.02 M $Ba(OH)_2 \cdot 8H_2O$] solution and placed in an oven at 200 °C for 24 hr. Final samples were then cleaned and dried to obtain vertically grown $BaTiO_3$ NW arrays on a Ti substrate.

Fabrication process for a $BaTiO_3$ single NW on a flexible substrate

A $BaTiO_3$ single NW-based PEH was fabricated using a previously reported procedure [15]. To form the electrode lines and pads on the flexible substrate, a 100 nm thick aluminum (Al) layer was deposited on a polyimide (PI) substrate (thickness of 125 μm) by radio frequency (RF) sputtering; the layer was then patterned using a standard microfabrication process. Then, a thin chromium (Cr) layer was deposited onto an Al electrode-coated flexible substrate to inhibit charging problems during the focused ion beam (FIB) process. A drop of $BaTiO_3$ NWs dispersed in ethanol was dropped onto the Al/PI substrates; as a result, the NWs placed between the Al electrode lines. Both ends of a single NW were connected to the Al line with an FIB-Pt electrode; two copper (Cu) wires were fixed with Al pads for output measurements.

Fabrication process for vertically grown $BaTiO_3$ NW arrays-based PEH

Figures 1a to 1d show schematic illustrations of fabrication process of a $BaTiO_3$ NW arrays-based PEH. The vertically grown $BaTiO_3$ NW arrays on a Ti substrate (Figure 1a) were coated with ultraviolet (UV) sensitive polyurethane (PU, Norland optical adhesive, No. 73) as an adhesive/dielectric layer and sandwiched between two transparent indium tin oxide (ITO) electrode-coated PET substrates; then, the PU layers were cured by UV light for 10 min (Figure 1b). As shown in Figure 1c, to measure the electric signals produced from a PEH, a conductive

https://doi.org/10.1557/adv.2017.305

epoxy (silver paste) was used to connect to two Cu wires to the two ITO electrode pads. Finally, the PEH was encapsulated using a polymeric polydimethylsiloxane (PDMS) elastomer (Figure 1d) and the poling process was conducted with a high electric field to enhance the piezoelectric performances.

Measurement of piezoelectric output signals

We used a customized bending machine that can uniformly deform energy devices to verify the output performance of an individual $BaTiO_3$ single NW. The electric output sources (open-circuit voltage and short-circuit current) generated from a stressed $BaTiO_3$ single NW were detected by a high-resolution measurement unit (Keithley 6514 Electrometer) and simultaneously recorded by a computer. When the vertically grown $BaTiO_3$ NW arrays-based PEH was bent by human fingers to harvest, we characterized the generated output voltage and current from an energy device.

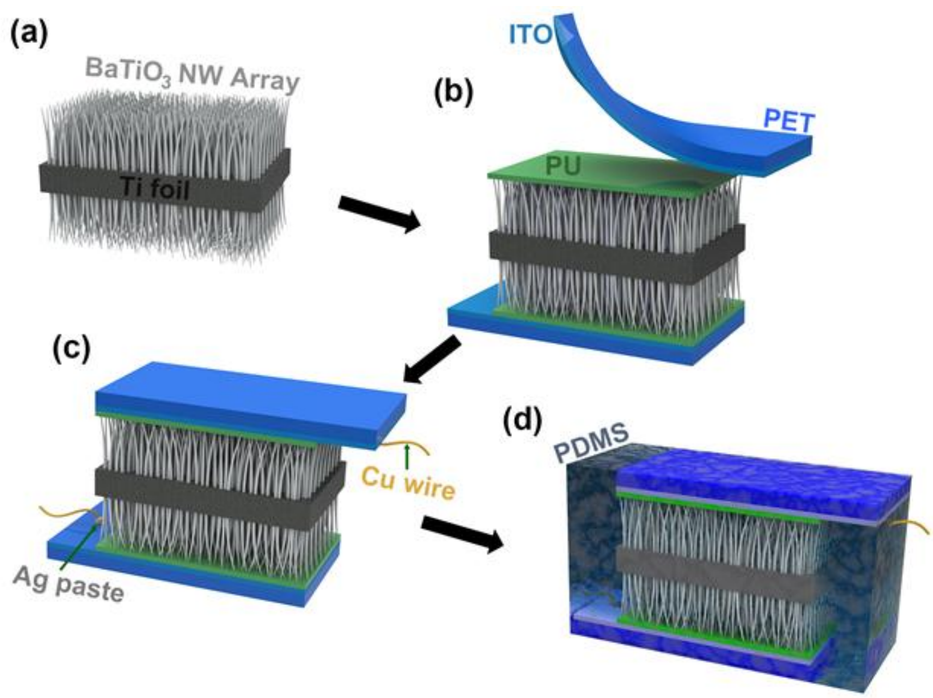

Figure 1. Schematic illustration of overall fabrication process of vertically grown $BaTiO_3$ NW arrays-based PEH. (a) Vertically grown NW arrays onto the top and bottom surfaces of a Ti substrate. (b) $BaTiO_3$ NW arrays sandwiched between two ITO electrode-coated PET substrates. (c) A $BaTiO_3$ NW arrays-based PEH connected to two Cu wires. (d) A PEH encapsulated with a PDMS elastomer.

RESULTS AND DISCUSSION

We carried out microstructural analysis to characterize the morphology and lengths of $BaTiO_3$ NWs on a Ti substrate (Figure 2a) using the field emission scanning electron microscopy (FE-SEM) (S-4800, HITACHI, Japan). The $BaTiO_3$ NWs showed lengths of about 15 μm. The detailed analysis of the crystallographic structure was performed using an X-ray diffraction

https://doi.org/10.1557/adv.2017.305

(XRD, RIGAKU, Ultima IV) unit with Cu Kα radiation operated at 40 kV and 40 mA. These results (XRD patterns from $BaTiO_3$ NW arrays on Ti substrate) were provided in Figure 2b and matched with the general results of perovskite-structured materials without peaks of by-products.

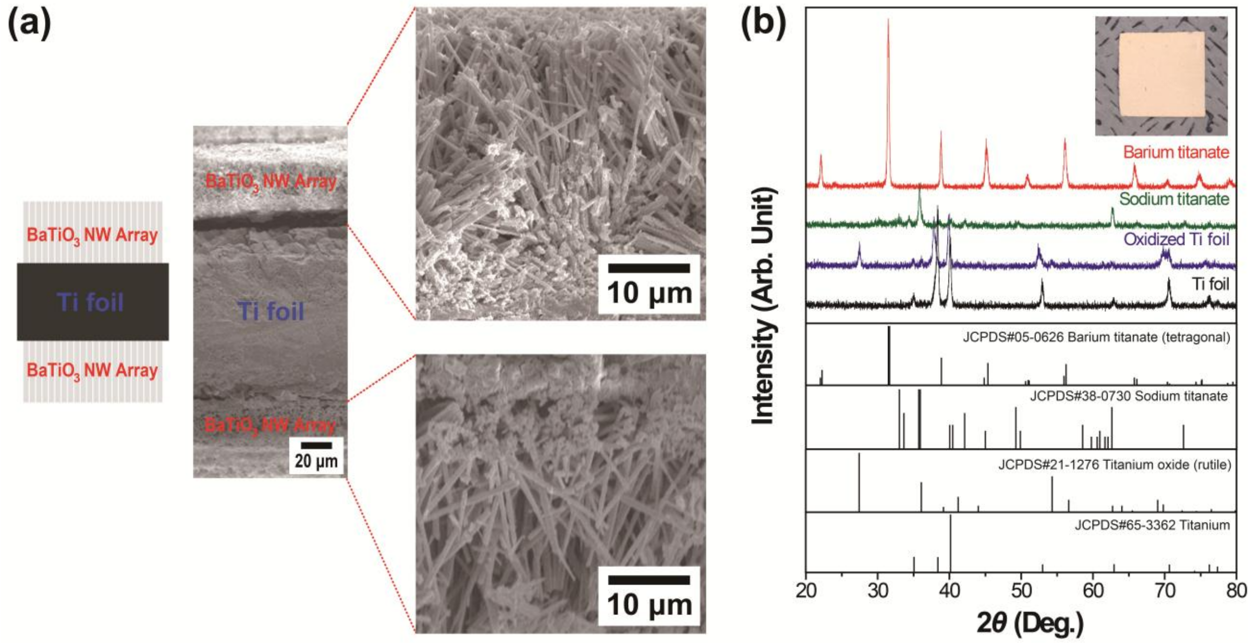

Figure 2. (a) The cross-sectional SEM images of $BaTiO_3$ NW arrays grown onto top and bottom surfaces of a Ti substrate. (b) XRD patterns of the resultants obtained from at each step.

To investigate the power generating ability of an individual NW in $BaTiO_3$ NW arrays, a $BaTiO_3$ single NW was taken from the arrays on the Ti substrate. Figure 3a shows a $BaTiO_3$ single NW (length of ~ 10 μm) transferred onto an Al patterned flexible substrate using a simple process detailed in the Experimental section. The $BaTiO_3$ single NW fixed with the Al electrode by FIB-Pt deposition process on a flexible PI substrate was longitudinally bent; then, the piezo-ceramics produced a piezo-potential between the two electrodes that acts as a driving force to move the electrons. Finally, we fabricated a $BaTiO_3$ single NW-based flexible PEH by connecting Cu wires to the Al pads and characterized the energy harvesting of an individual NW during periodically bending and unbending motions, as shown in Figure 3b which contained the captured photographs of the flexible PEH in bending and releasing states. When a $BaTIO_3$ single NW-based PEH on a flexible substrate was repeatedly stressed by a customized bending machine, the output voltage from 6 to 10 mV and current peaks from 1.0 to 2.3 nA were produced from a $BaTiO_3$ single NW, as shown in Figures 3c and 3d. These values were obtained by mechanical deformation with a strain of 0.283 % (corresponding to a bending radius of 2.20 cm) at a straining rate of 2.32 $\%\cdot s^{-1}$. Moreover, the switching polarity test was conducted to confirm that the measured output signals were the converted piezoelectricity from a $BaTiO_3$ single NW. Since the output values when connected in forward connection were similar to those of in reverse connection and the its polarity was inversed, we verified that the electric sources came from the piezoelectric energy materials.

https://doi.org/10.1557/adv.2017.305

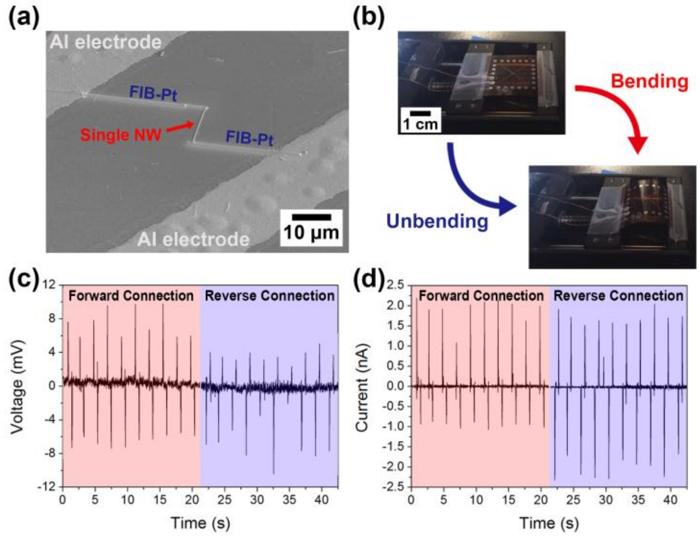

Figure 3. (a) SEM image of $BaTiO_3$ single NW transferred onto an Al patterned flexible substrate by FIB-Pt deposition process. (b) The captured photographs of a single NW-based flexible PEH after and before being deformed by a bending machine. The output voltage (c) and current pulse (d) generated from a $BaTiO_3$ single NW during mechanical bending/unbending motions in forward and reverse connections, respectively.

Figure 4a shows a fabricated NW arrays-based PEH embedded in a PDMS elastomer that was deformed by human fingers. By repetitive deflection of the energy device as shown in Figure 4b, the $BaTiO_3$ NWs on the Ti substrate were stressed by compressive force and individual NWs acted as an energy generation source. The piezoelectric potential induced between the top and bottom electrodes drives the electron flows and leads to the electric signals through an external circuit. The output performance of a fabricated NW arrays-based PEH is shown in Figures 4c and 4d. The maximum open-circuit voltage and short-circuit current were about 90 V and 1.2 μA, respectively; these values were obtained from an PEH with an activation area of 3 cm × 3 cm.

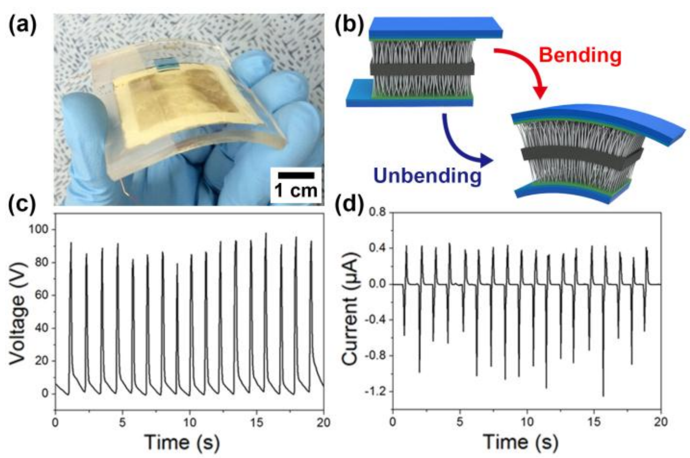

Figure 4. (a) Photograph of $BaTiO_3$ NW arrays-based PEH (3 cm × 3 cm) bent by human fingers. (b) Schematic of NW arrays-based PEH under original (releasing) and bending states. The output voltage (c) and current (d) converted from mechanical deformations by human fingers.

CONCLUSIONS

We synthesized the vertically grown $BaTiO_3$ NW arrays of a Ti substrate by adopting the two-step hydrothermal reactions for use in PEH that can convert electrical energy source from mechanical deformation. To evaluate the ability of individual NWs in power generation, a $BaTiO_3$ single NW that was taken from well-aligned NW arrays on a Ti foil was transferred onto a plastic substrate and fixed with electrode lines by FIB-Pt deposition process. During the periodic bending and unbending, output voltage from 6 to 10 mV and current peaks from 1.0 to 2.3 nA were generated from a single NW with length of 10 μm. To demonstrate piezoelectric energy harvesting from $BaTiO_3$ NW arrays, the piezoelectric arrays were sandwiched between two transparent electrode-coated PET films and then packaged with PDMS elastomer. Under mechanical bending motions by human fingers, the double $BaTiO_3$ nanowire arrays with an active area of 3 cm x 3 cm efficiently generated electric signals with the open-circuit voltage of 90 V and the short-circuit current of 1.2 μA; these harvested electric signals are superior to those of not only the ZnO nanowire arrays but also the single-side $BaTiO_3$ nanowire array-based PEHs.

ACKNOWLEDGMENTS

This work was supported by Gyeongnam National University of Science and Technology (GNTECH) Grant 2016.

REFERENCES

1. G. J. Aubrecht, *Energy: Physical, Environmental, and Social Impact*, 3rd ed. (Pearson Education, London, 2006) pp. 2-15.
2. S. Priya, D. J. Inman, *Energy Harvesting Technologies*. (Springer Science, New York, 2009).
3. Y. Qi and M. C. McAlpine, Energy Environ. Sci. **3**, 1275 (2010).
4. S. P. Beeby, M. J. Tudor and N. M. White, Meas. Sci. Technol. **17**, R175 (2006).
5. Z. L. Wang and J. Song, Science **312**, 242 (2006).
6. X. Wang, J. Song, J. Liu and Z. L. Wang, Science **316**, 102 (2007).
7. R. Yang, Y. Qin, L. Dai and Z. L. Wang, Nat. Nanotechnol. **4**, 34 (2009).
8. G. Zhu, R. Yang, S. Wang and Z. L. Wang, Nano Lett. **10**, 3151 (2010).
9. M. Y. Lu, J. Song, M. P. Lu, C. Y. Lee, L. J. Chen and Z. L. Wang, ACS Nano **3**, 357 (2009).
10. Y. F. Lin, J. Song, Y. Ding, S. Y. Lu and Z. L. Wang, Appl. Phys. Lett. **92**, 022105 (2008).
11. C. T. Huang, J. H. Song, W. F. Lee, Y. Ding, Z. Y. Gao, Y. Hao, L. J. Chen and Z. L. Wang, J. Am. Chem. Soc. **132**, 4766 (2010).
12. K.-I. Park, S. Xu, Y. Liu, G. T. Hwang, S. J. L. Kang, Z. L. Wang and K. J. Lee, Nano Lett. **10**, 4939 (2010).
13. K.-I. Park, J. H. Son, G.-T. Hwang, C. K. Jeong, J. Ryu, M. Koo, I. Choi, S. H. Lee, M. Byun, Z. L. Wang and K. J. Lee, Adv. Mater. **26**, 2514 (2014).
14. S. Xu, G. Poirier and N. Yao, Nano Lett. **12**, 2238 (2012).
15. B. Moorthy, C. Baek, J. E. Wang, C. K. Jeong, S. Moon, K.-I. Park and D. K. Kim, RSC Adv. **7**, 260 (2017).

https://doi.org/10.1557/adv.2017.305